CHEMISTRY
A European Journal

A Journal of
ChemPubSoc Europe

Accepted Article

Title: Arylazopyrazole photoswitches in aqueous solution: Substituent effects, photophysical properties and host-guest chemistry

Authors: Lucas Stricker, Marcus Bockmann, Thomas Kirse, Nikos Doltsinis, and Bart Jan Ravoo

To be cited as: *Chem. Eur. J.* 10.1002/chem.201800587

Link to VoR: http://dx.doi.org/10.1002/chem.201800587

Supported by
ACES

WILEY-VCH

10.1002/chem.201800587

WILEY-VCH

Arylazopyrazole photoswitches in aqueous solution: Substituent effects, photophysical properties and host-guest chemistry

Lucas Stricker[a], Marcus Böckmann[b], Thomas M. Kirse[a],Nikos L. Doltsinis[b] and Bart Jan Ravoo*[a]

Abstract: Arylazopyrazoles (AAPs) represent a new class of photochromic azo compounds offering high yield *E*/*Z*-isomerization in both directions by irradiation with UV or green light, respectively. Additionally, AAPs show a light-responsive host-guest interaction with *β*-cyclodextrin (CD) with comparable binding affinities as reported for azobenzenes. Substitution of one benzene of the azobenzene by a dimethylpyrazole leads to a separation of the *n*-*π** and *π*-*π** absorbances of the molecules enabling the optimized photochromic behavior. Since it is expected that AAPs show a strong dependence of the photophysical properties on the substitution pattern of the photochromic core, we herein report a comprehensive study on the effect of various substituents of water soluble AAPs. Therefore, substituents with different electronic and steric effects were introduced on different positions of AAP. The *E*/*Z*-isomerization, the half-life time of the Z-isomer, the quantum yields as well as the stability against glutathione (GSH) were investigated. Additionally, DFT calculations were conducted and the host-guest chemistry with *β*-cyclodextrin was investigated.

Introduction

Molecular switches are currently under intensive investigation in various fields of science. Especially, light-responsive molecules – photoswitches – are of particular interest.[1] Controlling the function of complex systems by light is attractive, since light is non-invasive for the system and can be applied with high spatial and temporal control.[2–4] Several photoswitches, such as azobenzenes[5–7], diarylethenes[8,9] and spiropyranes[10–12] have been widely investigated and optimized by different substitution patterns to fulfill the desired criteria. Among all these photoswitches, azobenzene is the most commonly used,[13,14] since it offers in addition to the reversible photoisomerization, a light-responsive host-guest interaction with cyclodextrins.[15,16] The light-responsive azobenzene/cyclodextrin interaction was first reported by UENO *et al.* and since then extensive research was done on the construction of light-responsive supramolecular systems using this phenomenon.[16,17] In view of their importance in photoswitchable materials, azobenzenes have been modified in various ways to tailor them for specific applications. To circumvent the use of UV-light for the *E*-*Z* isomerization, the groups of HECHT and WOOLLEY reported tetra-*ortho* substituted azobenzenes, for which both isomerizations could be triggered by visible or even near IR light.[18–22] These compounds are now examples for optimized light-responsive moieties for the use in biological systems.[23] Furthermore, other groups reported red-shifted azobenzenes and a bridged azobenzene with improved photoisomerization quantum yields.[24–28] With regard to the *ortho*-methoxy substituted azobenzene of WOOLLEY, SI WU and coworkers were able to show that this compound can still interact with *β*-cyclodextrin similarly to the unsubstituted azobenzene. While the rod-like *E*-isomer forms a stable 1:1 host-guest complex with *β*-CD, the twisted and more polar *Z*-isomer is not showing any interaction. By using this property, several red-light responsive supramolecular systems such as hydrogels were reported.[29,30] HECHT and coworkers reported in additional studies of the *ortho*-fluorinated azobenzenes that the substitution pattern of these compounds can highly affect their properties.[31] Similar effects have been reported for azobenzenes in many examples. For instance, the so called “push-pull azobenzenes” with electron donating as well electron withdrawing substituents show a reversal of the absorbance bands in the UV/vis spectrum.[6]

The optimization of the azobenzene photoswitch also inspired the investigation of azoheteroarenes. In general, in these compounds, one benzene ring of the azobenzene is substituted by a heterocycle changing the electronic as well as the steric properties of the molecules.[32,33] A first promising example was reported by the group of HERGES. They showed that azoindazoles present a complete *E*-*Z* isomerization, whereas the *Z*-*E* isomerization with only 55% is still insufficient.[34]

In 2014, arylazopyrazoles (AAPs) were introduced by FUCHTER and coworkers. These molecules show excellent photophysical properties with quantitative photoisomerization in both directions (for dimethylpyrazoles) and very long half-life times (for pyrazoles).[35] Later, our group was able to show that AAPs can be additionally used in CD-based supramolecular systems, exhibiting similar light-responsive interaction with *β*-CD as it is reported for azobenzenes.[36] In recent publications, our group reported several improved light-responsive systems using the new AAP/cyclodextrin motif to enable better photocontrol, where the photoswitching of azobenzene was restricting the function of the supramolecular system, such as particle assemblies, hydrogels or DNA compaction.[37–42]

Similar to azobenzenes, it is expected that for AAPs the properties of the photoswitch are strongly dependent on the substitution pattern of the molecule. A first study varying the heterocycle was reported by FUCHTER in 2017 supporting this expectation.[43] Since the heterocycle is not taking part in the

[a] L. Stricker, T. M. Kirse, Prof. B. J. Ravoo
Organic Chemistry Institute and Center for Soft Nanoscience,
Westfälische Wilhelms-Universität Münster
Corrensstrasse 40, 48149 Münster (Germany)
E-mail: b.j.ravoo@uni-muenster.de
[b] M. Böckmann, Prof. N. L. Doltsinis,
Institute for Solid State Theory and Center for Multiscale Theory & Computation
Westfälische Wilhelms-Universität Münster
Wilhelm-Klemm Str. 10, 48149 Münster (Germany)

Supporting information for this article is given via a link at the end of the document.

10.1002/chem.201800587

host-guest complexation of AAPs with *β*-CD the effect of substituents at the benzene ring is of particular interest for supramolecular systems using this interaction. Here, we report a comprehensive study of water-soluble AAPs substituted mainly at the benzene unit with special focus on the host-guest interaction, the switching behavior and the half-life time of the *Z*-isomer. In Figure 1 a schematic representation of the investigated AAPs **1-19** is shown. In addition, the quantum yields for the isomerization processes were determined and experimental results are supported by DFT calculations yielding predicted geometries and energy levels of the isomers together with barrier heights for thermal isomerization. For the potential use of AAPs *in vivo* the stability of these derivatives against concentrated GSH solution was investigated. Many azobenzenes show a rapid reduction of the N=N bond by GSH, including the *ortho*-methoxy azobenzenes of WOOLLEY.[20]

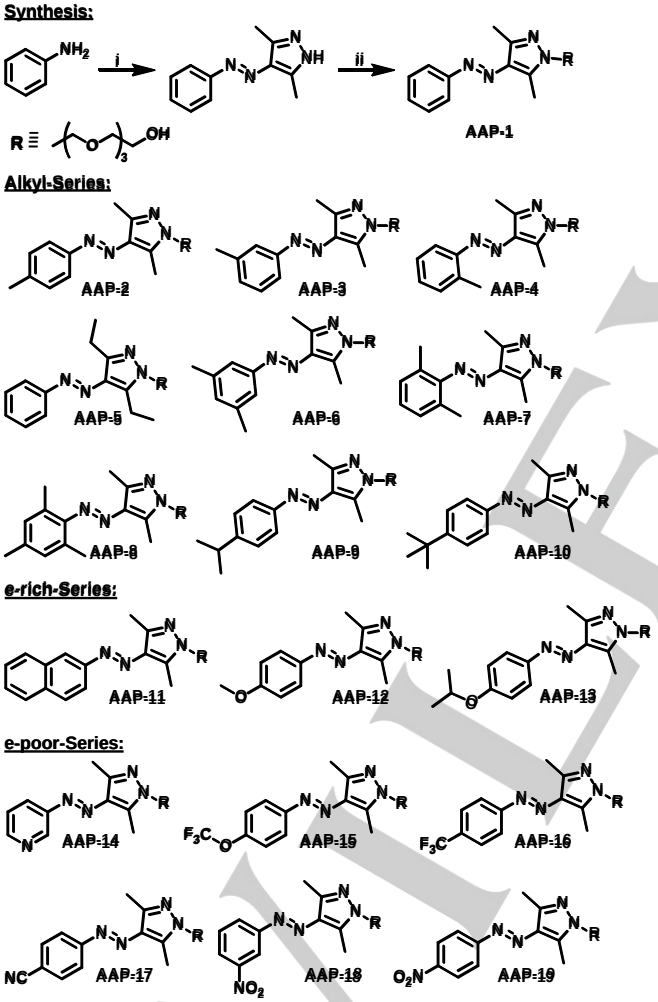

Scheme 1. Structures of all investigated AAPs **1-19** and schematic synthetic pathway shown exemplarily for **AAP-1**; **i:** 1) $NaNO_2$, HCl, AcOH, 2,4 pentadione (3,5 heptadione for **AAP-5**), NaOAc, H_2O/EtOH, 0°C → rt, 2 h, 28%-quant.; 2) $N_2H_4 \times xH_2O$, EtOH, Δ, 3 h, quant.; **ii:** TsOTEG, K_2CO_3, LiBr, ACN, Δ, 72 h, 9-99%.

Results and Discussion

Synthesis

AAPs **1-19** were synthesized using a standardized protocol. Starting from commercially available anilines each AAP was synthesized in a simple three step synthesis. The aniline was converted into the corresponding diazonium salt by hydrochloric acid and sodium nitrite, which was reacted *in situ* with 2,4 pentadione (3,5 heptadione for **AAP-5**) yielding the hydrazones as yellow precipitate without further purification. By refluxing with hydrazine hydrate the corresponding AAP was obtained in quantitative yields. To enhance the water solubility of all compounds a tetraethyleneglycol (TEG) chain was attached by *N*-alkylation of the pyrazole. Details of the synthesis and analysis of all AAPs are provided in the supporting information. The characteristic signals of the CH_3 group at the pyrazole around 2.5 ppm in the NMR-spectra indicate that in all cases the E-isomer represents the thermodynamically isomer.[35]

Photoswitching

All AAPs were investigated by UV/vis spectroscopy with regard to the switching behavior and the absorbance maxima of both isomers. The isomerization of AAPs is shown in Figure 1A. Light-induced switching was done in all cases for three cycles. Figure 1 (B, C, D and E) shows representative measurements for **AAP-1** and **AAP-7** and all spectroscopic information obtained by these measurements are summarized in Table 1 and 2 for all AAPs. Spectra for all compounds can be found in the supporting information (Figure S1-S17). Additionally, theoretical spectra calculated by DFT calculations (dashed lines) are plotted together with the experimental spectra for comparison.

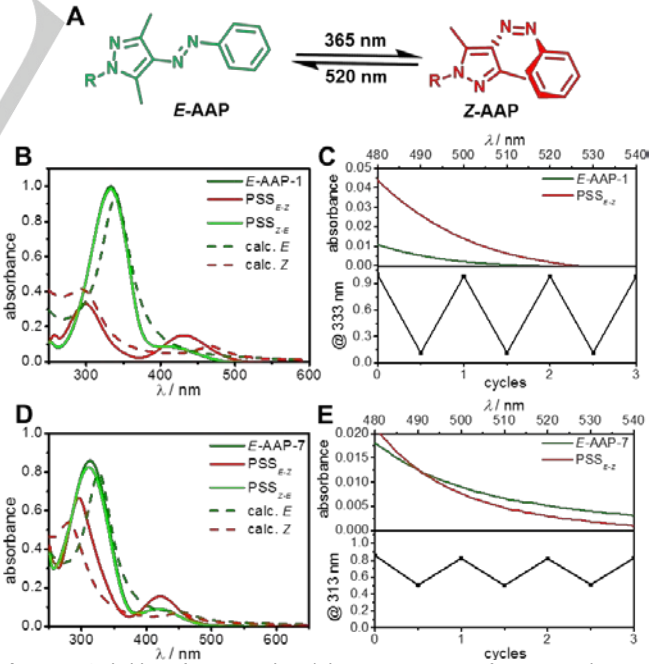

Figure 1. Switching of AAPs and UV/Vis-measurements of **AAP-1** and **AAP-7**; **A:** Light induced isomerization of AAPs **B/D:** Experimental normalized and calculated UV/Vis spectrum of the photoisomerization of **AAP-1** and **AAP-7** in water; **C/E:** Zoom-in at the 500 nm area (top) and absorbance at maximum for three switching cycles (bottom); **AAP-1** (c = 35 µmol) **AAP-7** (c = 50 µmol).

In general, all AAPs show the typical behavior upon irradiation with UV-light (365 nm) for *E*-*Z* isomerization and green light (520 nm) for *Z*-*E*-isomerization. UV irradiation leads to a blue-shift and intensity decrease of the *π*-*π** absorbance, whereas the intensity of the *n*-*π** absorbance increases and shows a slight red-shift for most compounds, which is characteristic for the isomerization from the thermodynamically stable *E*-isomer to the *Z*-isomer. A second irradiation with green light is retrieving the original spectrum with minimum 90% of original intensity, except for **AAP-4**, **AAP-7** (s. Figure 1D and E) and **AAP-8**. The positions of the absorbance maxima for both transitions as well as the difference of the maxima for both isomers are summarized in Table 1.

Table 1. Spectroscopic data of AAPs for *E*- and *Z*-isomer in water at 25°C; including the absorbance maxima (λ_{max}) and separation (Δ) for the $n\rightarrow\pi^*$ and the $\pi\rightarrow\pi^*$ transitions.

	$\pi\rightarrow\pi^*$ λ_{max} *E* [nm]	λ_{max} *Z* [nm]	Δ π→π* [nm]	$n\rightarrow\pi^*$ λ_{max} *E* [nm]	$n\rightarrow\pi^*$ λ_{max} *Z* [nm]	Δ n→π* [nm]
AAP-1	333	299	34	420	433	13
AAP-2	335	300	35	424	433	9
AAP-3	336	299	37	422	432	10
AAP-4	341	299	42	414	428	14
AAP-5	334	298	36	416	435	19
AAP-6	337	300	37	418	432	12
AAP-7	313	296	17	419	420	1
AAP-8	325	297	28	419	425	6
AAP-9	341	303	38	416	435	19
AAP-10	338	311	27	416	432	16
AAP-11	340	306	34	420	440	20
AAP-12	347	312	35	400	440	40
AAP-13	347	311	36	–	440	–
AAP-14	334	300	34	418	432	14
AAP-15	333	315	18	417	429	12
AAP-16	339	303	36	420	436	16
AAP-17	345	301	44	427	439	12
AAP-18	332	303	29	422	432	10
AAP-19	362	–	–	–	–	–

However, it was not possible to record a spectrum for the *Z*-isomer of the *p*-NO_2 substituted AAP (**AAP-19**). We assume that the strong electron withdrawing effect of the nitro group leads to a "push-pull system", which is known to cause unstable *Z*-isomers for azobenzene derivatives.[44] As a consequence the *Z*-isomer of **AAP-19** shows an extremely fast thermal relaxation to the *E*-isomer. For the remaining 18 derivatives reversible switching was induced for at least three cycles without any photobleaching.

Table 1 shows that substituents influence the positions of the absorbance maxima in certain cases. Strong electron withdrawing groups, such as nitrile or nitro group, in *para*-position cause a red-shift of the *π*-*π**-absorbance of the *E*-isomers. A similar effect is observed for the electron rich series AAPs **11-13**. For AAPs **10-13** and **15**, a red-shift of the *π*-*π**-absorbance of the *Z*-isomer is observed, whereas this band is not strongly affected for the remaining AAPs. Another interesting feature is the blue-shift of the *n*-*π**-absorbance for the *ortho*-substituted AAPs **7** and **8** resulting in rather low separation of this absorbance for both isomers, which results in poor switching already observed in the UV/Vis-spectra (Figure 1D and E).

The photostationary state (PSS) of AAPs and other azo compounds in general is determined primarily by the possibility of selective excitation of one isomer. The difference in the absorbance maxima stated in Table 1 clearly shows that the substitution affects the peak splitting and therefore gives a first hint on the PSS. Moreover, the key feature of the excellent switching of AAPs is the forced twisted conformation of the *Z*-isomer by the methyl groups at the pyrazole breaking the symmetry and increasing the intensity of the *n*-*π**-absorbance. By this, this band absorbs at wavelengths >500 nm where the *E*-isomer does not absorb, thus allowing exclusive *n*-*π**-excitation.

In addition to the absorbance maxima discussed above, the extinction coefficients at the irradiation wavelength were determined (Table 2). In this way, a more meaningful assumption on the exclusive excitation of on isomer over the other might be drawn for every AAP. The collected data clearly shows that in all cases higher extinction of *E*-isomers at 365 nm is observed, which enables the *E*-*Z*-isomerization by irradiation with UV-light of this wavelength. For most AAPs ε of the *Z*-Isomer is at this wavelength approximately 10 times smaller. In contrast to this a lower difference is observed for AAPs **8**, **10**, **15** and **18**, which can cause lower $PSS_{E\text{-}Z}$ for these compounds. With regard to ε at 520 nm *E*-isomers of AAPs **1**, **2**, **6**, **9** and **12** show no absorbance at all, which should enable exclusive excitation of the *Z*-isomer and high $PSS_{Z\text{-}E}$. In addition for most AAPs a significant larger extinction coefficient is found for the *Z*-isomers, whereas ε for the *E*-isomers are in general rather low. In this case again the results found for the *ortho*-substituted compounds **4**, **7** and **8** show a discrepancy from the other AAPs. For these compounds comparable extinction coefficients for both isomers at 520 nm were determined. This is in agreement with the previous findings of the spectroscopic data shown in Table 1 and Figure 1 further supporting the assumption of low $PSS_{Z\text{-}E}$ for these AAPs due to fully overlapping absorbances. This phenomenon limits the photoisomerization in unmodified azobenzenes. In addition, the extinction coefficients at the absorbance maxima were determined and can be found in the supporting information (Table S1).

Table 2. Determined extinction coefficients (ε) of AAPs **1-19** at the irradiation wavelength in water.

	ε_{365nm} *E* [$M^{-1}cm^{-1}$]	ε_{365nm} *Z* [$M^{-1}cm^{-1}$]	ε_{520nm} *E* [$M^{-1}cm^{-1}$]	ε_{520nm} *Z* [$M^{-1}cm^{-1}$]
AAP-1	11400	800	0	60
AAP-2	11800	1400	0	150
AAP-3	11200	1300	80	460
AAP-4	12100	1300	200	180
AAP-5	7500	700	20	110
AAP-6	11000	1100	0	110
AAP-7	13500	1200	100	20
AAP-8	4600	1100	5	20
AAP-9	14000	800	0	140
AAP-10	13500	3400	50	160
AAP-11	21000	2200	20	290
AAP-12	31100	1500	0	380
AAP-13	18800	1100	30	310
AAP-14	13000	1400	50	210
AAP-15	8500	2600	20	100
AAP-16	13600	900	20	170
AAP-17	16200	1500	60	300
AAP-18	11400	3400	10	120
AAP-19	25700	–	230	–

Furthermore, the quantum yields for the photoisomerization were determined and stated in the supporting information (Figures S18-S35 and Table S1). The collected values in this case vary over a broad range and no obvious trends could be found. However the measurements show that for all cases the photoisomerization is complete in a time scale of a few minutes.

To finally quantify the photoisomerization, the PSS were determined by ^{1}H-NMR spectroscopy. A first spectrum was recorded before irradiation with 365 nm light to yield $PSS_{E\text{-}Z}$ and recording a second spectrum. After irradiation with 520 nm light a third spectrum of the $PSS_{Z\text{-}E}$ was recorded. Figure 2 shows a zoom-in of the aromatic region for the measurements made for **AAP-12** as an example. The full spectra for **AAP-12**, as well as full spectra and zoom-ins in the areas used for integration can be found in the supporting information (Figures S36-S70). The determined PSS are listed in Table 3. For some AAPs with strong hydrophobic character a broadening of the signals in the *E*-isomer can be observed due to aggregation of the AAP core in aqueous solution, but nevertheless the PSS could be determined reliably.

The PSS measurements confirmed the results obtained by UV/Vis spectroscopy. **AAP-4**, **AAP-7**, **AAP-8** and **AAP-18** show in comparison to the other AAPs poor photoswitching. Except for the four AAPs mentioned before, the remaining AAPs show excellent PSS of at least 90% in both directions caused by increased absorbance above 500 nm and good separation of the peaks. Especially **AAP-3** (*m*-Me), **AAP-12** (*p*-OMe), **AAP-13** (*p*-O*i*Pr) and **AAP-*15*** (*p*-OCF_3) show remarkable photoswitching with quantitative isomerization in both directions. However the obtained results do not fully correlate with the extinction coefficients in Table 2, since from these four compounds only **AAP-12** showed no absorbance at 520 nm. In summary these findings show that additional substituents can further improve the PSS of the AAP photoswitch.

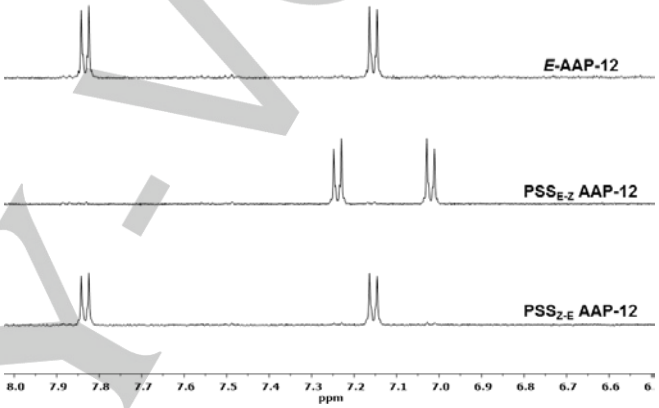

Figure 2. Aromatic region of the ^{1}H-NMR spectra for PSS determination of **AAP-12**; recorded in D_2O, c = 200 µM, irradiation times: 30 min.

In the cases of **AAP-4** and **AAP-18**, photoisomerization efficiency is excellent in one direction (93% for *E*-*Z* of **AAP-4** and 92% for *Z*-*E* of **AAP-18**), whereas the photoisomerization of the full *ortho*-substituted AAPs **7** and **8** is less efficient in both directions (only 70-80%). The explanation for the incomplete photoswitching of these compounds can be found by a close inspection of the UV/Vis spectra and the calculated structures of these compounds. The absorbances for in the UV/Vis spectra of **AAP-7** and **AAP-8** show a near complete overlap limiting selective excitation (Figures S6 and S7 and Table 2). The overlap is due to the geometric structure of these compounds. By the additional methyl groups in the *ortho*-positions of the benzene ring the *E*-isomer tends to twist due to steric hindrance. The slightly distorted structure breaks the symmetry in the N=N double bond increasing the intensity of the *n*-π^*-absorbance. For **AAP-18** in similar fashion a low difference in the extinction coefficients at 365 nm was observed explaining the findings from the PSS measurements.

Another interesting aspect is that in contrast to all the other AAPs, **7** and **8** exhibit a considerable amount of the thermodynamically unstable *Z*-isomer directly after sample preparation (~30%). A possible explanation might be stabilizing London dispersion interactions of the substituents in the *Z*-isomer. This hypothesis is corroborated by our theoretically determined relative energies (see Table 4 below). SCHWEIGHAUSER *et al*. reported that bulky alkyl substituents affect the stability of the *Z*-isomer by steric hindrance, but that

additionally stabilizing dispersion interactions play an important role and can stabilize the *Z*-isomer.[45] This should also lead to longer half-life times of ***Z*-AAP-7** and **Z-AAP-8**.

Table 3. Photostationary state (PSS) of AAPs determined by NMR-spectroscopy in D_2O at 25°C (*c* = 200 µM), irradiation time: 30 min.

	$PSS_{E\text{-}Z}$	$PSS_{Z\text{-}E}$		$PSS_{E\text{-}Z}$	$PSS_{Z\text{-}E}$
AAP-1	92%	90%	**AAP-11**	94%	>98%
AAP-2	>98%	92%	**AAP-12**	>98%	>98%
AAP-3	98%	96%	**AAP-13**	>98%	96%
AAP-4	93%	79%	**AAP-14**	93%	92%
AAP-5	94%	90%	**AAP-15**	97%	>98%
AAP-6	>98%	90%	**AAP-16**	>98%	90%
AAP-7	68%	69%	**AAP-17**	92%	90%
AAP-8	83%	68%	**AAP-18**	80%	92%
AAP-9	>98%	90%	**AAP-19**	-	-
AAP-10	>98%	90%			

Thermal stability

Another important feature for molecular switches is the thermal stability of the metastable state. Depending on desired application longer or shorter half-life times are preferred. For example for storage of optical data – a research field currently dominated by diarylethenes – a long half-life time is preferred.[2,9] Therefore, we investigated the thermal stability of AAPs **1-19** by time dependent UV/Vis spectroscopy. The results are summarized in Figure 3 and the measurements can be found in the supporting information (Figure S71-S79).

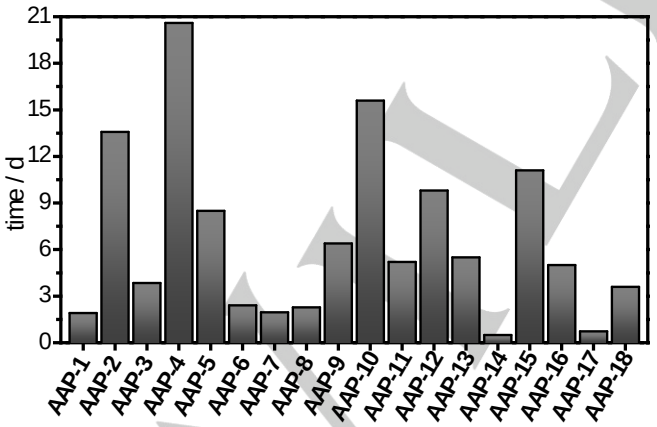

Figure 3. Half-life times of AAPs **1-18** in *dd*H_2O at 25°C (70°C for **AAP-7** and **AAP-8**).

Figure 3 and the result found before for **AAP-19** show that the half-life time of *Z*-AAPs can vary between a few seconds (**AAP-19**), a few hours (**AAP-14** and **AAP-17**), to days or even multiple month and years (**AAP-7** and **AAP-8**). As expected the *ortho*-substituted AAPs **4**, **7** and **8** show the longest half-life time, which might be explained by enhanced dispersion interactions. Whereas $T_{1/2}$ for **AAP-4** was determined to be ~21 days at room temperature, for **AAP-7** and **AAP-8** no thermal relaxation was observed after 3 months. As a consequence the half-life time of these compounds was determined at 70°C yielding $T_{1/2}$ of ~2 days. This value is close to the longest reported value of azobenzenes, which was reported by HECHT and coworkers for *ortho*-fluorinated azobenzenes (95 h at 60°C = ~700 days at rt) and unsubstituted AAPs (1000 days at rt).[31,35]

With regard to the half-life times of the different AAPs, the following trends emerge. It appears from our data that *para*- and *ortho*-substitution affect the half-life time more strongly in comparison to *meta*-substitution (**AAP-3** and **AAP-6**). Substitution with electron withdrawing groups (EWGs) at the *para*-position leads to an increased life-time for a weak withdrawing effect (**AAP-15**, OCF_3), but if the EWG effect is increased a drastic decrease of life time is observed correlating with the HAMMETT coefficient of the substituents **AAP-19** < **AAP-17** < **AAP-16** < **AAP-15** (NO_2 ($\sigma = 0.78$), CN ($\sigma = 0.66$), CF_3 ($\sigma = 0.54$), OCF_3 ($\sigma = 0.35$). For electron donating (EDG) substituents, a higher thermal stability is observed, the highest for **AAP-12** (OMe). Comparison of **AAP-5** and **AAP-1** again shows that London dispersion effects may contribute to the stabilization of the *Z*-isomer, since they increase from methyl to ethyl substituents. Additionally, increasing the *para*-substituents from methyl to *tert*-butyl (increased inductive effect) leads to an increased half-life time (with isopropyl as exception). To summarize, the half-life time of AAPs can be manipulated over a wide time scale by introducing specific substituents at selected positions.

DFT calculations

To further support our initial assumptions, (TD)DFT calculations were carried out for all AAPs. To reduce computational demand, the TEG chain was substituted by a methyl group for the calculations. In addition to the already mentioned theoretical UV/Vis spectra, the relative energies of the two isomers and the T-shaped transition state were computed together with the corresponding optimized geometries. All computational details, the determined geometries and the energy profiles along the ground state isomerization path can be found in the supporting information (Figures S80-S98 and Table S2). Table 4 summarizes the energies of the *Z*-isomer and the transition state relative to the *E*-isomer for all AAPs **1-19**.

The calculated relative energies further support the findings of the thermal stability for the *Z*-isomers. AAPs **4**, **7** and **8** show the lowest energies for the *Z*-isomer, resulting in a higher thermal stability of the metastable *Z*-isomer.

Another correlation can be found for the thermal stability of the EWG substituted AAPs. The relative energies of the transition states decrease in the same order as it was observed for the thermal stability. In doing so, the total relative energy (i.e. the activation barrier for thermal relaxation) decreases from around 1.7 eV for **AAP-15** (OCF_3) *via* **AAP-16** (CF_3,~1.6 eV), **AAP-17** (CN, 1.45 eV) to 1.3 eV for **AAP-19** (NO_2). Comparison of the values for **AAP-19** and **AAP-18** (1.3 eV vs. 1.6 eV) again

verifies the dominant influence of substituents at the *para*-position over the *meta*-position.

Table 4. Relative energies of *Z*-isomer (*Z*) and transition state (TS) determined by DFT calculations for AAPs **1-19**.

	Rel. E (*Z*) [eV]	Rel. E (TS) [eV]		Rel. E (*Z*) [eV]	Rel. E (TS) [eV]
AAP-1	0.656	1.763	**AAP-11**	0.679	1.794
AAP-2	0.660	1.798	**AAP-12**	0.668	1.889
AAP-3	0.652	1.755	**AAP-13**	0.669	1.894
AAP-4	0.578	1.681	**AAP-14**	0.673	1.728
AAP-5	0.678	1.752	**AAP-15**	0.664	1.695
AAP-6	0.650	1.776	**AAP-16**	0.658	1.580
AAP-7	0.527	1.548	**AAP-17**	0.663	1.464
AAP-8	0.534	1.612	**AAP-18**	0.675	1.638
AAP-9	0.657	1.789	**AAP-19**	0.658	1.301
AAP-10	0.656	1.797			

The transition state energy of the fully meta-substituted **AAP-6** is higher than the fully ortho-substituted **AAP-7** and **8**.This may be explained by London dispersion interactions of **AAP-7** and **8** mentioned before. The assumption for the incomplete photoswitching of the *ortho*-substituted AAPs is also verified by the optimized geometries and the resulting dihedral angles (Table S2). While the *E*-isomer of all other AAPs shows a fully planar structure with both aromatic rings in plane with the N=N bond (NNCC ≈ 0°), the *E*-isomer of **AAP-4**, **AAP-7** and **AAP-8** shows a twisted conformation, where the aromatic rings are out of plane. While the pyrazole is only slightly twisted (NNCC ≈ 3°-5°) the benzene ring is twisted by 20° to 38°. A comparison of the *E*-isomers of **AAP-1** and **AAP-7** is pictured in Figure 4.

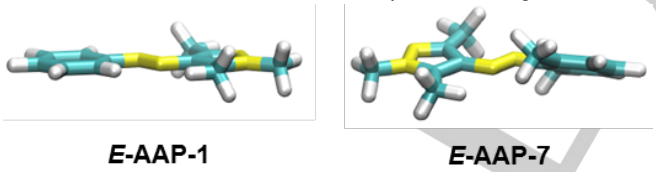

Figure 4. Comparison of optimized geometries for **AAP-1** and **AAP-7**.

Host-guest chemistry

In our previous publication we have already demonstrated that the unsubstituted AAPs form a light-responsive host-guest inclusion complex with *β*-CD (Figure 5).[36] The determined binding constant (K [M^{-1}]) of ***E*-AAP-1** (Table 4) is similar to the reported binding constant of azobenzene and *β*-CD (~2000 M^{-1}).[46] Additionally, the binding affinity is drastically decreased by isomerization upon irradiation with UV-light (365 nm). The binding constant of ***Z*-AAP-1** determined by ITC drops down to about 700 M^{-1}, which is again in good agreement with the reported value of *Z*-azobenzene (~500 M^{-1}).[47] The reduced affinity of *Z*- vs. *E*-isomers will be amplified in highly multivalent systems such as particle assemblies or polymers.[39] The slightly higher binding affinity of *Z*-AAP in contrast to *Z*-azobenzenes might be attributed to the more twisted conformation of AAPs compared to azobenzenes (dihedral angle (CNNC) = 4.2° vs 12.2°, Table S2).[48–50] As a result the benzene ring is more exposed and therefore more easily accessible for the *β*-CD.

In general, the binding affinities of guests for *β*-CD are mainly driven by the hydrophobic effect and dominated by two parameters. Firstly, the space filling of the cavity by the guest molecule to maximize the dispersion interactions by optimal fit. Secondly, high energy water has to leave the cavity and the solvation shell of the guest and enter the bulk water, yielding additional hydrogen bonding.[51] A schematic representation of the host-guest chemistry between AAPs and *β*-CD in aqueous solution is shown in Figure 5.

We investigated the binding affinities of the substituted AAPs to

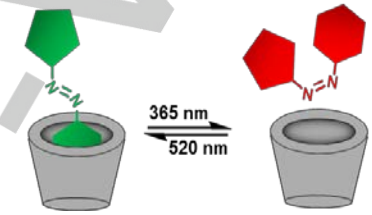

Figure 5. Schematic representation of the light-responsive host-guest interaction of AAPs and *β*-cyclodextrin.

β-CD with the aim to maximize the binding constant, but at the same time to maintain the light-response of this interaction. Therefore, additional isothermal titration calorimetry measurements of AAPs **2-19** with *β*-CD were carried out and the determined binding constants (K) are summarized in Table 5. Furthermore, if a significant binding constant was found for the *E*-isomer an additional measurement was performed for an irradiated sample analyzing the interaction of the *Z*-isomer. Exemplarily, the measurements for ***E*-** and ***Z*-AAP-12** are shown in Figure 6. The remaining measurements can be found in the supporting information (Figures S99-S108).

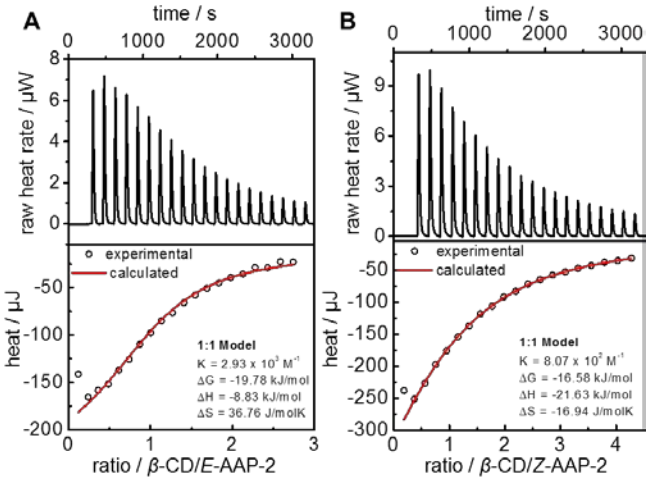

Figure 6. ITC titration curve and the corresponding fit of **AAP-12; A: *E*-AAP-2** (1 mM) and **B: *Z*-AAP-2** (1 mM) with *β*-CD (10 mM) in ddH_2O.

ITC measurements reveal that the binding affinity strongly depends on the substitution pattern at the benzene ring of the AAPs. As expected, the introduction of polar units, such as pyridine (**AAP-14**), nitrile (**AAP-17**), as well as fluorinated substituents OCF_3 for (**AAP-15** and CF_3 (**AAP-16**) drastically reduce the binding affinity. These findings are consistent with the observation that fluorinated or polar guests show significant lower binding affinities to cyclodextrins.[52]

In contrast the titration of the *p*-NO_2-substituted compound (**AAP-19**), shows a remarkable binding affinity of ~5000 M^{-1}. While varying the position of the nitro group to the *meta*-position (**AAP-18**), it yields no detectable interaction of the AAP with *β*-CD. These findings lead us to the conclusion that the *p*-nitro group might "slide" through the cavity of the cyclodextrin and protrude from the cavity (allowing secondary interactions with the rim of the CD) and only the benzene of **AAP-19** is located in the interior of the CD. This arrangement is not possible for **AAP-18** since the nitro group is located at the *meta*-position and, as a consequence, no interaction is found.

Table 5. Binding constants of AAPs with *β*-CD determined by isothermal titration calorimetry (ITC) in ddH_2O; c = 1 mM (AAP) and 10 mM (*β*-CD).

	K [M^{-1}]		K [M^{-1}]
***E*-AAP-1**	1.3 x 10^3	***E*-AAP-10**	3.96 x 10^4
***Z*-AAP-1**	7.02 x 10^2	***Z*-AAP-10**	1.76 x 10^4
***E*-AAP-2**	2.93 x 10^3	***E*-AAP-11**	-
***Z*-AAP-2**	8.07 x 10^2	***E*-AAP-12**	1.74 x 10^3
***E*-AAP-3**	2.06 x 10^2	***Z*-AAP-12**	8.09 x 10^2
***E*-AAP-4**	9.55 x 10^1	***E*-AAP-13**	8.80 x 10^3
***E*-AAP-5**	2.12 x 10^3	***Z*-AAP-13**	1.12 x 10^3
***Z*-AAP-5**	5.02 x 10^2	***E*-AAP-14**	1.90 x 10^2
***E*-AAP-6**	-	***E*-AAP-15**	3.24 x 10^2
***E*-AAP-7**	5.27 x 10^2	***E*-AAP-16**	2.22
***E*-AAP-8**	-	***E*-AAP-17**	3.38 x 10^2
***E*-AAP-9**	3.18 x 10^4	***E*-AAP18**	-
***Z*-AAP-9**	5.47 x 10^3	***E*-AAP-19**	5.04 x 10^3

Focusing on the alkyl-substituted AAPs, there is a clear trend that a *para*-substitution is highly favored over substitution in *ortho*- or *meta*-positions. Whereas the *ortho*- and *meta*-substituted AAPs (**3**, **4**, and **6-8**) show negligible binding affinities, *para*-substitution leads to a clear trend with increasing binding constants from H < OMe < Me < O*i*Pr < *i*Pr < *t*Bu (**AAP-1** < **AAP-12** < **AAP-2** < **AAP-13** < **AAP-9** < **AAP-10**). The same trend was already observed for substituted benzoic acids yielding similar binding affinities.[53] In this way, the binding constant of *E*-AAPs could be tuned within a range of 1000 M^{-1} and 40000 M^{-1}. The higher affinity of *para*-substituted AAPs over the substitution at other positions can be explained by the more rod-like structure of *para*-substituted AAPs resulting in a better fit of the guests inside the cavity. The slightly higher binding affinity of **AAP-5** might be explained by secondary interactions of the ethyl groups with the outer rim of the cyclodextrin, since previous studies showed that the pyrazole unit is not participating in the host-guest complexation.[36] Interestingly, the naphthalene AAP (**AAP-11**) did not show a host-guest complexation with *β*-CD which was in contrast to our expectations. Nevertheless, **AAP-11** might be an interesting candidate for cyclodextrins with larger cavities such as *γ*-CD. On the other hand, the spectacularly high binding constants of **AAP-9** (~30000 M^{-1}) and **AAP-10** (~40000 M^{-1}) drew our attention, possessing the highest affinities reported for azo compounds so far. However, measurements of the *Z*-isomers still show, in both cases, a significant binding constant to *β*-CD, meaning a loss of the light-responsive characteristic of the host-guest interaction. Probably the isopropylphenyl and *tert*-butylphenyl residues are still accessible for the *β*-CD in the *Z*-isomer leading to the formation of an inclusion complex. Other than these two, the rest of the AAPs show a low binding affinity for the *Z*-isomer compared to the *E*-isomer. **AAP-13** (*p*-*i*OPr) would appear best suited for supramolecular systems, since it shows a large difference in the binding affinity (~9000 M^{-1} (*E*) vs. ~1000 M^{-1}(*Z*)). For the remaining binding AAPs **2**, **5** and **12**, they show the same binding affinity as the unsubstituted **AAP-1** for the *Z*-isomers allowing their incorporation in light-triggered host-guest systems.

Glutathione stability

Despite the need of UV-light for the *E*-*Z*-isomerization of AAPs, they might have potential applications in biological applications and first examples of AAPs in DNA based systems have already been reported.[38,41] For the use of azo based photoswitches in *in vivo* applications, their stability in the reducing cellular environment, containing compounds such as glutathione (GSH), is crucial. It is known that some azo compounds undergo photobleaching by the reduction of the N=N bond by GSH depending on their structure and redox potential.[54,55] The reduction of diazenylcarboxylic acids by GSH was investigated by KOSOWER *et al.*, who show that reduction occurs via a nucleophilic attack of the thiol at one nitrogen following a protonation of the second nitrogen.[56] WOOLLEY and coworkers assumed that the reduction of the tetra *ortho*-methoxy azobenzene involves an initial protonation of one nitrogen, facilitating the attack of the thiol. The intermediate is stabilized by hydrogen bonding with the *ortho*-methoxy substituent.[19] In contrast to the *ortho*-methoxy azobenzenes, *ortho*-chloro or *ortho*-thiol substituted derivatives are stable in concentrated GSH solution, due to the absence of hydrogen bonding.

We investigated the stability of AAPs **1-19** in a concentrated GSH solution (10 mM, highest cellular concentration of GSH). Therefore, solutions of all AAPs were incubated with GSH and in different intervals UV/Vis spectra were recorded. The measured spectra can be found in the supporting information (Figures S109- S115). As a result, we found almost no photobleaching of

any *E*-AAPs showing excellent stability against GSH for at least 22 h (Figure 5). In comparison, the *ortho*-methoxy azobenzenes are reduced relatively fast at the same conditions ($\tau_{1/2}$ = 1 h).[19] In our case, only **AAP-10** and **11** show a minimal change in the UV/Vis-spectra, whereas the remaining AAPs show no degradation at all. An explanation for the stability of *E*-AAPs might be the higher electron density of the N=N bond by the electron rich pyrazole hindering the nucleophilic attack of the thiol. Prior protonation is not favored in this case, since there is no possibility for additional stabilization by hydrogen bonds. An additional stabilizing effect might be steric hindrance by the methyl groups of the pyrazole. In summary, AAPs possess excellent stability against GSH and therefore are a promising candidate for *in vivo* applications.

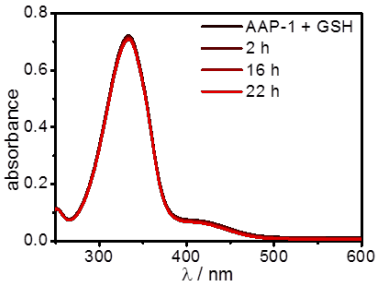

Figure 7. Stability test of **AAP-1** (c = 33 µM) against concentrated GSH (10 mM) for 22 h.

Conclusions

In this paper, we report how the substitution pattern of the benzene ring determines the characteristics of the AAP photoswitch. AAPs **1-19** used in this study were synthesized in a facile three-step synthesis. All AAPs showed excellent photoisomerization, which is crucial for the switching of highly multivalent supramolecular systems. Exceptional cases are AAPs bearing *ortho*-substituents at the benzene ring. Additionally, it was possible to tune the thermal stability of AAPs over a broad timescale from several seconds to days, months and years. By increasing the rod-like structure of AAPs by introduction of non-polar substituents in *para*-position the binding affinity of AAPs to *β*-cyclodextrin could be increased to 40000 M^{-1}. However, a too high binding constant leads to a loss in the light-response of this interaction. Nevertheless, AAPs **2**, **5**, **12** and **13** are examples for improved AAPs with increased binding affinities for the *E*-isomers, without showing a significant interaction in the *Z*-isomer. Last but not least, the outstanding stability against glutathione allows their potential application *in vivo*. This is a clear advantage compared to most azobenzenes. All in all, this study documents the superior characteristics of the AAP based molecular switch. Since azoheteroarene photoswitches have not been investigated in great detail until now our findings should stimulate the further study, development and application of azoheteroarene photoswitches in different fields of science.

Experimental Section

Below general information regarding synthesis, instruments and measurements is stated. More detailed information can be found in the supporting information.

Synthesis of AAPs 1-19

General procedure I: Synthesis of 3-(2-phenylhydrazono)pentane-2,4-diones[36]

$NaNO_2$ (1.2 eq.) dissolved in a minimum amount of water was added dropwise to a solution of aniline (1.0 eq.) in AcOH (1.5 mL/mmol) and HCl (12 M, 0.23 mL/mmol) at 0 °C. After stirring for 45 minutes the resulting diazonium salt was transferred to a suspension of pentane-2,4-dione (1.3 eq.) and NaOAc (3 eq.) in EtOH (1 mL/mmol) and water (0.6 mL/mmol). The mixture was stirred for 1 h and the resulting yellow precipitate was collected *via* vacuum filtration. After washing with water and water/EtOH (1:1), the obtained solid was dried under vacuum affording the desired compound.

General procedure II: Synthesis of arylazopyrazoles[36]

Hydrazine x hydrate (1 eq.) was added to a solution of desired 3-(2-phenylhydrazono)pentane-2,4-dione (1 eq.) or heptane-3,5-dione dissolved in EtOH and refluxed for 3 hours. Concentration under reduced pressure yielded the resulting arylazopyrazole without further purification.

General procedure III: Coupling of arylazopyrazoles to TsO-TEG-OH[39]

The arylazopyrazole (1 eq.) was dissolved in dry ACN. K_2CO_3 (5 eq.), TsO-TEG-OH (1.1 eq.) and LiBr (cat.) were added. The heterogeneous mixture was refluxed for 36 h. Afterwards the solvent was removed under reduced pressure, the resulting residue was dissolved in EtOAc/H_2O (1:1) and the layers were separated. The organic layer was washed with H_2O and brine (2 ×). Then, the organic layer was dried over $MgSO_4$ and the solvent was removed under vacuum. The crude product was purified by column chromatography (SiO_2, DCM/MeOH 97:3).

UV/Vis spectroscopy

UV/Vis measurements were conducted by using a JASCO V-650 double-beam spectrophotometer (JASCO Labor- und Datentechnik GmbH, Gross-Umstadt) at 25 °C, using 1 mL low-volume disposable PMMA cuvettes (Brand GmbH & CO KG, Wertheim). The spectrometer was controlled by Spectra Manager version 2.08.04 (Jasco Labor- und Datentechnik GmbH, Gross-Umstadt). The samples were dissolved in an appropriate solvent and measured against the same solvent. Data analysis was carried out using OriginPro 9.1G (OriginLab Corp., Northampton, Massachusetts, USA).

Photoswitching

Two different light sources were utilized for photoswitching experiments, a 365 nm UV LED Gen2 Emitter (LZ1-00UV00) from LEDENGIN (365 nm) for *E-Z*- isomerization and a LSC-G HighPower-LED emitting at 520 nm for *Z-E*-isomerization. Irradiation times are stated at corresponding measurements section.

Isothermal titration calorimetry (ITC)

ITC was carried out using a TA Instruments Nano ITC Low Volume (Waters Corp., Milford, Massachusetts, USA) with a cell volume of 170 µL using ITCRun Version 2.1.7.0 Firmware version 1.31 (TA Instruments, WatersCorp., Milford, Massachusetts, USA). All titrations were performed using a 50 µL syringe and 20 injections of 2.5 µL at a temperature of 25 °C with a stirring rate of 350 rpm while titrating the CD to the AAP solution. All samples were prepared in ddwater and degassed for 10 min before use. The data were analyzed using NanoAnalyse Data Analysis version 2.36 (TA Instruments, Waters Corp., Milford, Massachusetts, USA), Microsoft® Excel version 14.07113.5005 as part of Microsoft® Office Professional Plus 2010 (Microsoft Corp., Redmond, Washington, USA) and OriginPro 9.1.G (OriginLab Corp., Northampton, Massachusetts, USA). Before analysis, all data were corrected by subtraction of a blank titration of the CD into pure solvent.

Acknowledgements

This work was funded by the Volkswagen Foundation and the Deutsche Forschungsgemeinschaft DFG (EXC 1003). We thank Dr. Klaus Bergander for help with the NMR measurements for PSS determination and Matthias Hayduk for support with the synthesis.

Keywords: Molecular switches • photoswitches • substitution effect • arylazopyrazoles • host-guest chemistry • cyclodextrins• density functional theory

[1] B. L. Feringa, W. R. Browne, *Molecular Switches*, Wiley-VCH Verlag GmbH & Co. KGaA, **2011**.
[2] J. Zhang, Q. Zou, H. Tian, *Adv. Mater.* **2013**, *25*, 378–399.
[3] C. Brieke, F. Rohrbach, A. Gottschalk, G. Mayer, A. Heckel, *Angew. Chem. Int. Ed.* **2012**, *51*, 8446–8476; *Angew. Chem.* **2012**, *124*, 8572–8604.
[4] M. M. Russew, S. Hecht, *Adv. Mater.* **2010**, *22*, 3348–3360.
[5] P. Weis, S. Wu, *Macromol. Rapid Commun.* **2017**, 1700220.
[6] H. M. D. Bandara, S. C. Burdette, *Chem. Soc. Rev.* **2012**, *41*, 1809–1825.
[7] E. Léonard, F. Mangin, C. Villette, M. Billamboz, C. Len, *Catal. Sci. Technol.* **2016**, *6*, 379–398.
[8] M. Irie, *Chem. Rev.* **2000**, *100*, 1685–1716.
[9] H. Tian, S. Yang, *Chem. Soc. Rev.* **2004**, *33*, 85–97.
[10] R. Klajn, *Chem. Soc. Rev.* **2014**, *43*, 148–84.
[11] B. S. Lukyanov, M. B. Lukyanova, *Chem. Heterocycl. Compd.* **2005**, *41*, 281–311.
[12] G. Berkovic, V. Krongauz, V. Weiss, *Chem. Rev.* **2000**, *100*, 1741–1754.
[13] E. Merino, *Chem. Soc. Rev.* **2011**, *40*, 3835–3853.
[14] S. Yagai, T. Karatsu, A. Kitamura, *Chem. Eur. J.* **2005**, *11*, 4054–4063.
[15] R. Klajn, *Pure Appl. Chem.* **2010**, *82*, 2247–2279.
[16] D. H. Qu, Q. C. Wang, Q. W. Zhang, X. Ma, H. Tian, *Chem. Rev.* **2015**, *115*, 7543–7588.
[17] A. Ueno, K. Takahashi, T. Osa, *J. Chem. Soc., Chem. Commun.* **1980**, 837–838.
[18] D. Bléger, J. Schwarz, A. M. Brouwer, S. Hecht, *J. Am. Chem. Soc.* **2012**, *134*, 20597–20600.
[19] S. Samanta, A. A. Beharry, O. Sadovski, T. M. McCormick, A. Babalhavaeji, V. Tropepe, G. A. Woolley, *J. Am. Chem. Soc.* **2013**, *135*, 9777–9784.
[20] S. Samanta, T. M. McCormick, S. K. Schmidt, D. S. Seferos, G. A. Woolley, *Chem. Commun.* **2013**, *49*, 10314–10316.
[21] A. A. Beharry, O. Sadovski, G. A. Woolley, *J. Am. Chem. Soc.* **2011**, *133*, 19684–19687.
[22] M. Dong, A. Babalhavaeji, C. V. Collins, K. Jarrah, O. Sadovski, Q. Dai, G. A. Woolley, *J. Am. Chem. Soc.* **2017**, *139*, 13483–13486.
[23] M. Dong, A. Babalhavaeji, S. Samanta, A. A. Beharry, G. A. Woolley, *Acc. Chem. Res.* **2015**, *48*, 2662–2670.
[24] D. Bléger, S. Hecht, *Angew. Chem. Int. Ed.* **2015**, *54*, 11338–11349; *Angew. Chem.* **2015**, *127*, 11494–11506.
[25] Y. Yang, R. P. Hughes, I. Aprahamian, *J. Am. Chem. Soc.* **2012**, *134*, 15221–15224.
[26] R. Siewertsen, H. Neumann, B. Buchheim-Stehn, R. Herges, C. Näther, F. Renth, F. Temps, *J. Am. Chem. Soc.* **2009**, *131*, 15594–15595.
[27] M. Böckmann, N. L. Doltsinis, D. Marx, *J. Chem. Phys.* **2012**, *137*, 22A505.
[28] M. Böckmann, N. L. Doltsinis, D. Marx, *Angew. Chem. Int. Ed.* **2010**, *49*, 3382-3384; *Angew. Chem.* **2010**, *122*, 3454-3456.
[29] D. Wang, M. Wagner, H.-J. Butt, S. Wu, *Soft Matter* **2015**, *11*, 7656–7662.
[30] D. Wang, S. Wu, *Langmuir* **2016**, *32*, 632–636.
[31] C. Knie, M. Utrecht, F. Zhao, H. Kulla, S. Kovalenko, A. M. Brouwer, P. Saalfrank, S. Hecht, D. Bléger, *Chem. Eur. J.* **2014**, *20*, 16492–16501.
[32] R. Travieso-Puente, S. Budzak, J. Chen, P. Stacko, J. T. B. H. Jastrzebski, D. Jacquemin, E. Otten, *J. Am. Chem. Soc.* **2017**, *139*, 3328–3331.
[33] J. Garcia-Amorós, M. C. R. Castro, P. Coelho, M. M. M. Raposo, D. Velasco, *Chem. Commun.* **2013**, *49*, 11427–11429.
[34] C. Schütt, G. Heitmann, T. Wendler, B. Krahwinkel, R. Herges, *J. Org. Chem.* **2016**, *81*, 1206–1215.
[35] C. E. Weston, R. D. Richardson, P. R. Haycock, A. J. P. White, M. J. Fuchter, *J. Am. Chem. Soc.* **2014**, *136*, 11878–11881.
[36] L. Stricker, E.-C. Fritz, M. Peterlechner, N. L. Doltsinis, B. J. Ravoo, *J. Am. Chem. Soc.* **2016**, *138*, 4547–4554.
[37] N. Möller, T. Hellwig, L. Stricker, S. Engel, C. Fallnich, B. J. Ravoo, *Chem. Commun.* **2017**, *53*, 240–243.
[38] J. Moratz, L. Stricker, S. Engel, B. J. Ravoo, *Macromol. Rapid Commun.* **2018**, *38*, 1700256.
[39] S. Sagebiel, L. Stricker, S. Engel, B. J. Ravoo, *Chem. Commun.* **2017**, *53*, 9296–9299.
[40] C.-W. Chu, B. J. Ravoo, *Chem. Commun.* **2017**, *53*, 12450–12453.
[41] A. Volker, D. K. Prusty, M. Centola, Š. Marko, H. Jeffrey, J. Valero, K. Bernhard, M. Famulok, *Chem. Eur. J.* **2017**, DOI 10.1002/chem.201705500.
[42] S. Engel, N. Möller, L. Stricker, M. Peterlechner, B. J. Ravoo, *Small* **2018**, DOI: 10.1002/smll.201704287.
[43] J. Calbo, C. E. Weston, A. J. P. White, H. S. Rzepa, J. Contreras-García, M. J. Fuchter, *J. Am. Chem. Soc.* **2017**, *139*, 1261–1274.
[44] A. A. Beharry, G. A. Woolley, *Chem. Soc. Rev.* **2011**, *40*, 4422.
[45] L. Schweighauser, M. A. Strauss, S. Bellotto, H. A. Wegner, *Angew. Chem. Int. Ed.* **2015**, *54*, 13436–13439; *Angew. Chem.* **2015**, *127*, 13636–13639.
[46] S. K. M. Nalluri, J. Voskuhl, J. B. Bultema, E. J. Boekema, B. J. Ravoo, *Angew. Chem. Int. Ed.* **2011**, *50*, 9747-9751; *Angew. Chem.* **2011**, *123*, 9921–9925.
[47] L. Zhang, H. Zhang, F. Gao, H. Peng, Y. Ruan, Y. Xu, W. Weng, *RSC Adv.* **2015**, *5*, 12007–12014.
[48] T.-T. Yin, Z.-X. Zhao, H.-X. Zhang, *New J. Chem.* **2017**, *41*, 1659–1669.
[49] A. Cembran, F. Bernardi, M. Garavelli, L. Gagliardi, G. Orlandi, *J. Am. Chem. Soc.* **2004**, *126*, 3234–3243.
[50] M. Böckmann, N. L. Doltsinis, D. Marx, *J. Phys. Chem. A* **2010**, *114*, 745–754.
[51] E. M. M. Del Valle, *Process Biochem.* **2004**, *39*, 1033–1046.
[52] M. M. Becker, B. J. Ravoo, *Chem. Commun.* **2010**, *46*, 4369–4371.
[53] T. Höfler, G. Wenz, *J. Incl. Phenom. Macrocycl. Chem.* **1996**, *25*, 81–84.
[54] W. G. Levine, *Drug Metab. Rev.* **1991**, *23*, 253–309.
[55] A. A. Beharry, L. Wong, V. Tropepe, G. A. Woolley, *Angew. Chem. Int. Ed.* **2011**, *50*, 1325–1327; *Angew. Chem.* **2011**, *123*: 1361–

1363.
[56] E. M. Kosower, H. Kanety-Londner, *J. Am. Chem. Soc.* **1976**, *98*, 3001–3007.

10.1002/chem.201800587

WILEY-VCH

Entry for the Table of Contents

FULL PAPER

Substituted arylazopyrazoles (AAPs) are investigated as supramolecular photoswitches in aqueous solution. Selective photostationary states as well as improved binding affinities to *β*-cyclodextrin are found. Our experimental findings are supported by DFT calculations.

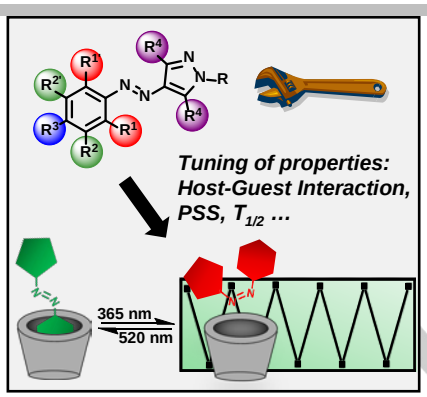

*Lucas Stricker, Marcus Böckmann, Thomas M. Kirse, Nikos L. Doltsinis and Bart Jan Ravoo**

Page No. – Page No.

Arylazopyrazole photoswitches in aqueous solution: Substituent effects, photophysical properties and host-guest chemistry